


Study of hydraulic characteristics of trapezoidal piano key side weir using different approaches

Zeyneb Kilic ^{a,*} and M. Emin Emiroglu^b

^a Engineering Faculty, Department of Civil Engineering, Istanbul Aydin University, 34295 Istanbul, Turkey

^b Engineering Faculty, Department of Civil Engineering, Firat University, 23119, Elazig, Turkey

*Corresponding author. E-mail: zeyneboybay@gmail.com

ABSTRACT

Side weirs are widely used in hydraulic engineering applications. The studies on the subject have been generally focused on classical and labyrinth side weirs. However, the same is not true for piano key side weirs (PKSW) in a straight channel. The piano key weir (PKW) has high discharge capacity compared with classical weirs. In this study, the hydraulic characteristics of a trapezoidal piano key side weir (TPKSW) in straight channels were investigated experimentally. In all experiments, the hydraulic characteristics of nine TPKSW models were studied extensively using the De Marchi, Domínguez and Schmidt approaches in the subcritical flow regime, with Froude number range $0.12 < F_1 < 0.87$. The results show that a TPKSW provides better performance compared to traditional rectangular and triangular labyrinth side weirs. Specifically, for the $0.12 < F_1 < 0.4$ condition, the efficiencies of a TPKSW and trapezoidal labyrinth side weir are close to each other. A trapezoidal labyrinth side weir is more efficient than a TPKSW at larger Froude numbers. The discharge capacity of the TPKSW is 2.9 to 12 times higher than that of the rectangular side weir. Scatter diagrams were obtained for C_{PW} and F_1 numbers using various approaches available in the literature. The diagram generated by the De Marchi approach has much less scattering, compared to the diagrams generated by the Domínguez and Schmidt approaches. It has been determined that TPKSWs are an effective type of side weir in lateral flows. Lastly, an empirical equation was obtained for the discharge coefficient, which is in good agreement with the experimental data.

Key words: discharge coefficient, open-channel flow, piano key weir, side weir, water discharge

HIGHLIGHTS

- TPKSWs provide better discharge performance compared to traditional rectangular and triangular labyrinth side weirs.
- Most effective parameters discharge coefficient of TPKSW are Froude number and piezometric head.
- CFD methods successfully model TPKSW structures and provide consistent results with experimental data.
- The Schmidt and Domínguez methods produce very similar results. The De Marchi method provides less scatter data.

NOTATIONS

b	width of main channel (L)
B	length of sidewall of PKW (L)
B_i	downstream overhang length of PKW (L)
B_o	upstream overhang length of PKW (L)
C_d	side weir discharge coefficient (-)
C_{PW}	PKSW discharge coefficient (-)
E	specific energy (L)
F_1	Froude number at upstream end of side weir (-)
F_2	Froude number at downstream end of side weir (-)
g	acceleration due to gravity (LT^{-2})
h_1	piezometric head on side weir at upstream end (L)
h_2	piezometric head on side weir at downstream end (L)
y	the depth of flow at the section x (L)
y_1	flow depth at upstream end of side weir at channel center (L)
y_2	flow depth at downstream end of side weir at channel center (L)
W	opening length of side weir (L)

This is an Open Access article distributed under the terms of the Creative Commons Attribution Licence (CC BY 4.0), which permits copying, adaptation and redistribution, provided the original work is properly cited (<http://creativecommons.org/licenses/by/4.0/>).

W_i	inlet key width of PKW (L)
W_o	outlet key width of PKW (L)
V_1	flow velocity on the first edge of the weir (LT^{-1})
T_s	wall thickness of PKW (L)
L	total weir crest length of labyrinth and piano key side weir (L)
N_u	number of PKW-units (-)
P	height of weir crest (L)
σ	water surface tension (N/m)
Q	discharge in the main channel before m^3/s beginning of side weir (L^3T^{-1})
Q_1	total discharge in main channel at upstream end of side weir (L^3T^{-1})
Q_2	total discharge in main channel at downstream end of side weir (L^3T^{-1})
Q_w	outflow weir discharge (L^3T^{-1})
q	discharge per unit length over side weir (L^2T^{-1})
α	sidewall angle of the trapezoidal piano key and labyrinth side weir ($^\circ$)
α'	kinetic energy correction coefficient (-)
Φ	varied flow function of De Marchi (-)
δ	head angle ($^\circ$)
η	outflow efficiency (-)
χ	dimensionless ratio dependent on downstream hydraulic conditions (-)
φ	angle of the flow deviation ($^\circ$)

1. INTRODUCTION

Side weirs are often used to divert a certain amount of discharge from an open channel. Important hydraulic structures such as irrigation systems, wastewater facilities, sewerage networks, hydroelectric facilities and flood reduction or prevention networks often require components for efficient flow distribution and control. For this purpose, side weirs provide a spatially variable flow with decreasing discharge in the direction of the flow. In addition to directing water, another purpose of the side weirs is to measure the amount of discharge. The hydraulic characteristics of a side weir change depend on the type of weir, its cross-section, and the plan shapes of the main channel.

Since the hydraulic properties of a side weir depend on the type of weir, the subject still attracts the attention of researchers. Many important studies on classical sharp-crested weirs have been reported in the literature (Subramanya & Awasthy 1972; El-Khashab & Smith 1976; Ranga Raju *et al.* 1979; Kumar & Pathak 1987; Hager 1987; Borghei *et al.* 1999; Emiroglu *et al.* 2011; Ghaderi *et al.* 2020). The discharge coefficient equations for a conventional side weir, according to Subramanya and Awasthy (Subramanya & Awasthy 1972), Hager (Hager 1987) and Borghei *et al.* (1999) are given in Equations (1)–(3), respectively:

$$C_d = 0.864 \left(1 + F_1^2 - \frac{F_1^2}{2} \right)^{0.5} \quad (1)$$

$$C_d = 0.485 \left(\frac{2 + F_1^2}{2 + 3F_1^2} \right)^{0.5} \quad (2)$$

$$C_d = 0.70 - 0.48F_1 - 0.30 \left(\frac{P}{y_1} \right) + 0.06 \left(\frac{W}{b} \right) \quad (3)$$

There have been several experimental (Emiroglu *et al.* 2007; Borghei *et al.* 2013; Nezami *et al.* 2015) and numerical (Aydin & Emiroglu 2013, 2016; Abbasi *et al.* 2020) studies on labyrinth side weirs which indicated high performance and discharge

capacity. *Borghei et al. (2013)* studied a triangular labyrinth side weir with two cycles and proposed Equation (4):

$$C_d = \frac{-0.269 \cdot \left(\frac{W}{b \cdot \sin\left(\frac{\delta}{2}\right)}\right)^{-1.188} + \left(\frac{P}{y_1 - P}\right)^{0.18}}{1 + 0.649 \cdot \left(\frac{1}{\sin\left(\frac{\delta}{2}\right)}\right)^{-0.505} + 0.056 \cdot \left(\frac{F_1}{\sin\left(\frac{\delta}{2}\right)}\right)^{-1.275}} \quad (4)$$

where C_d is the discharge coefficient of the side weir (dimensionless), W is the opening length of the side weir (m), b is the channel width (m), δ is the head angle (degree), P is the crest height (m), y_1 is the depth of flow at the upstream end of the side weir in the main channel center line (m) and F_1 is the Froude number.

An extensive experimental study on a trapezoidal labyrinth side weir with two cycles was reported in *Emiroglu et al. (2014)*. The coefficient of discharge for this structure is given by:

$$C_d = \left[-0.001F_1^{-1.78} + 0.10\left(\frac{W}{b}\right)^{0.22} - 2.036\left(\frac{y_1 - P}{P}\right)^{0.05} + 2.82\left(\frac{L}{W \cdot \sin \alpha}\right)^{0.02} \right]^{5.77} \quad (5)$$

where L is the overflow length of the side weir (m) and α is the sidewall angle (degrees).

The first theoretical study on the hydraulics of a rectangular side weir was reported by *De Marchi (1934)* and is widely used for different types of side weirs (*Subramanya & Awasthy 1972; El-Khashab & Smith 1976; Hager 1987; Borghei et al. 1999; Borghei & Parvaneh 2011; Emiroglu et al. 2014*). Other approaches that are of limited use were proposed by Schmidt (*Borghei & Parvaneh 2011*) and *Domínguez (1935)*. *Emiroglu & Ikinciogullari (2016)* showed that the Schmidt approach provides valid results for discharge coefficient of classical rectangular side weirs. *Bagheri et al. (2014a, 2014b)* stated that the *Domínguez* approach is a reasonable method to determine the discharge coefficient of side weirs.

The piano key weir (PKW) is a particular shape of labyrinth weir involving up stream and downstream overhangs, to reduce the base length requirement (*Figure 1*). The PKW represents the evolution of the traditional labyrinth weir. Based on the slopes of inlet and outlet keys, the structure has a specific upstream and downstream overhang. This design reduces the footprint of the side weir compared to a rectangular labyrinth weir with vertical walls. As a result, the forces acting on the lateral walls are reduced, and the structural cost is reduced (*Kabiri-Samani & Javaheri 2012*). Therefore, in addition to the improved hydraulic performance, the PKW can be built even in very restricted foundation space, for example in the case of gravity dam

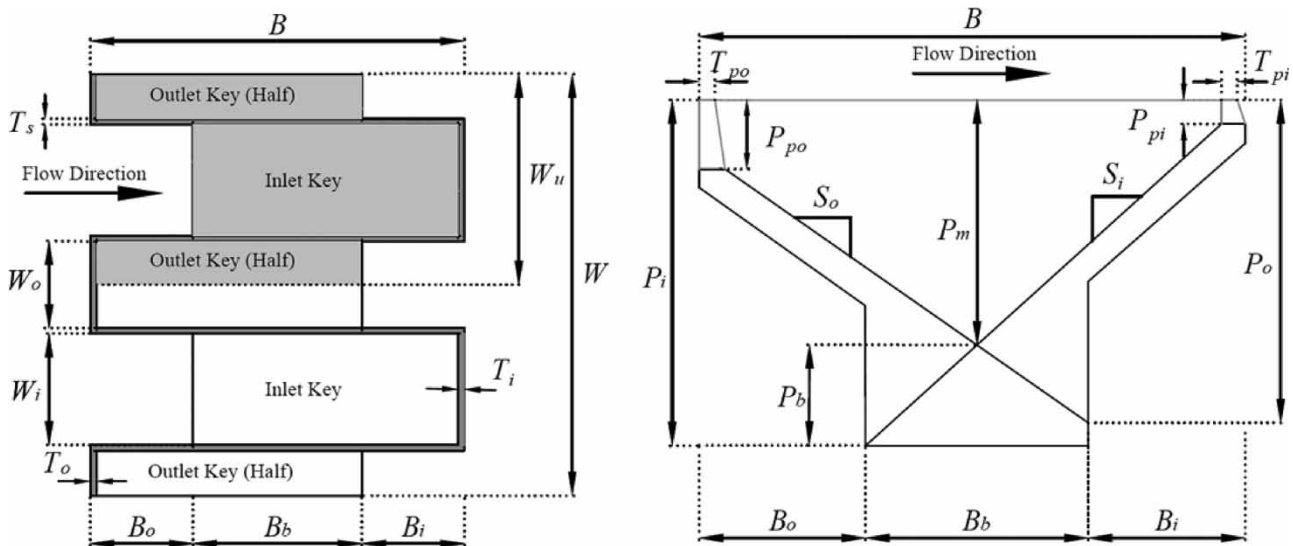


Figure 1 | Fundamental parameters of a PKW and unit PKW – plan view (left) and cross-section (right).

crests. For a given upstream head, the PKW may improve the discharge capacity by up to four times, compared to an ogee-crested weir of the same width (Ouamane & Lempérière 2006), and by 10% compared to a labyrinth weir of the same crest footprint (Anderson & Tullis 2011).

Various studies have been carried out in order to determine the best values for geometric characteristics that influence the efficiency of PKW as a frontal weir. The L/W ratio is the major parameter influencing discharge capacity, according to Ouamane & Lempérière (2006). Leite Ribeiro *et al.* (2012) stated that L/W value should be between 4 and 7, with $L/W = 5$ being the best. According to Lempérière *et al.* (2011), a L/W ratio of 5 is a good compromise between weir efficiency and structure complexity. Anderson & Tullis (2013) examined the performance of PKW with inlet–outlet key ratios ranging from 0.67 to 1.5 and found that increasing W_i/W_o (the inlet key width to the outlet key width) enhances flow coefficient. The best input and output key widths ratio, according to Lempérière *et al.* (2011), is between 1.2 and 1.5. Ouamane & Lempérière (2006) showed that the discharge efficiency depends on the P/W_u ratio and stated that when the weir height was increased by 20%, the discharge increase was between 5 and 10%. Gharibvand *et al.* (2016) stated that when the height of the PKW weir was increased by 50%, the flow efficiency increased by 26% at low nappe load values, thus supporting the relevant study.

The ‘PKW-unit’ represents the smallest extent of a complete structure of a PKW, comprising two transversal walls, two half outlets and an inlet. The basic geometric parameters of a PKW are the number of PKW-units (N_u), weir height (P), lateral crest length (B), up stream and downstream overhang lengths (B_o and B_i), inlet and outlet widths (W_i and W_o), and the wall thickness (T_s) (Pralong *et al.* 2011).

Depending on the existence of the upstream and downstream overhangs, PKW has been classified into four types, as presented in Figure 2. The basic geometry of a PKW, called type A, includes up stream and downstream overhangs. When the structure does not have a downstream or upstream overhang, the PKW is of type B or C, respectively. A PKW without overhangs is called type D (Lempérière *et al.* 2011). The structure is composed of two units placed along the side of a straight rectangular channel, in a fixed-bed (see Figure 3).

Studies on PKWs as side weirs are limited in the literature. Karimi *et al.* (2018) studied a C-type rectangular PKSW (RPKSW) in a straight channel. The study showed that C-type RPKSWs and rectangular labyrinth side weirs are more efficient than the equivalent linear side weirs, in terms of discharge capacity. Saghari *et al.* (2019) examined A-type trapezoidal piano key side weirs (TPKSWs) in a curved channel. As a result, an empirical equation is proposed to determine the discharge coefficient of A-type TPKSW. In an experimental study, Mehri *et al.* (2018) compared the discharge coefficient of C-type RPKSWs for channel curve angles of 30° and 120° in plan. The structure with 120° provides a higher weir discharge coefficient. In addition, Mehri *et al.* (2020) reported that P/h_1 is the most effective parameter on the discharge coefficient of the side weir with the A, B, C and D type piano keys in the 120° curved channel and stated that the most efficient model is the B type.

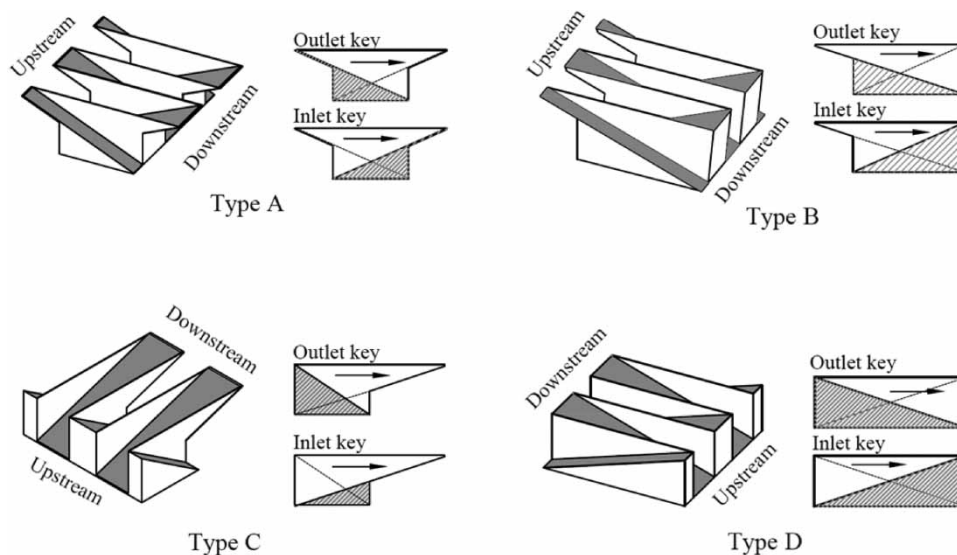


Figure 2 | Types of PKW.

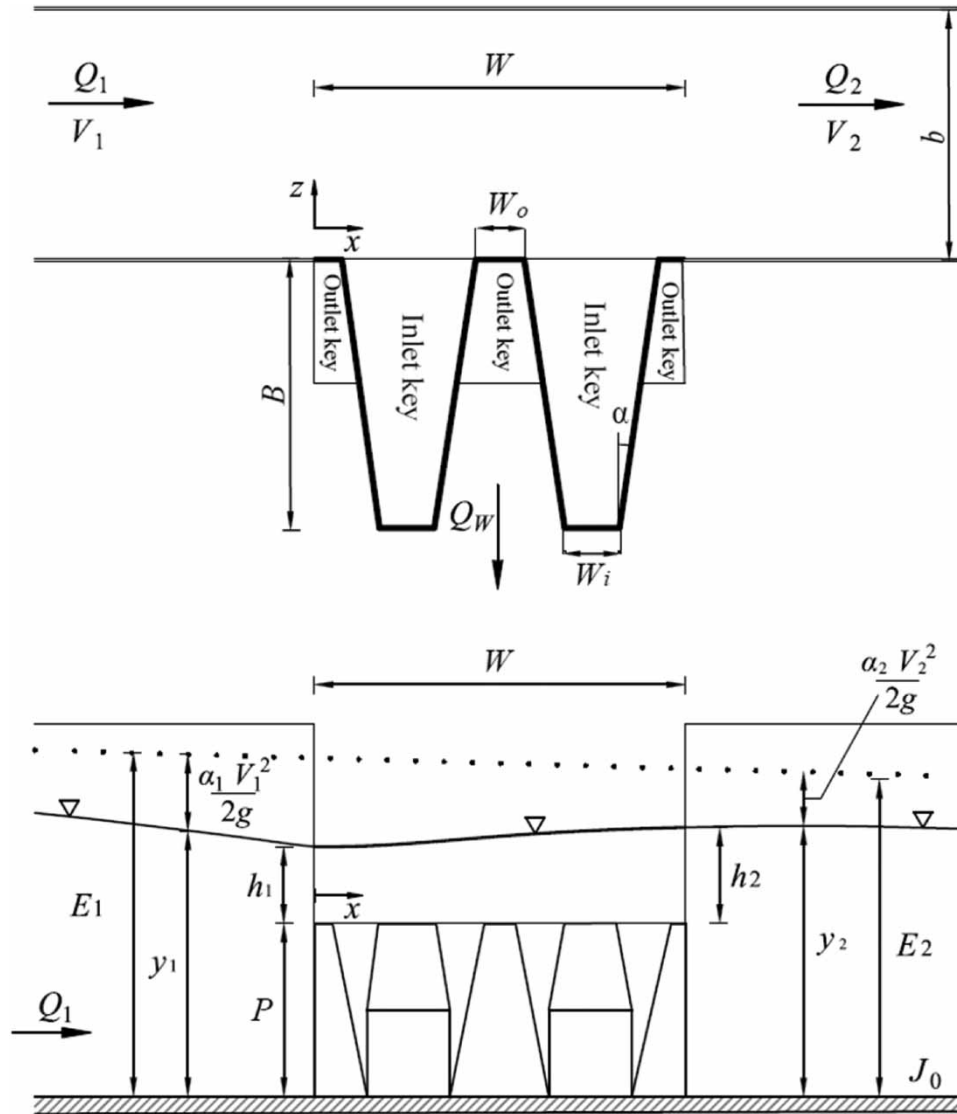


Figure 3 | Schematic layout of TPKSW: (a) plan, (b) front view.

Although TPKSW has been implemented in a curved channel, it has not yet been studied for a wide range of experiments as a side weir in a straight channel. The present study contributes to this by presenting experiments on the performance of a TPKSW. A wide range of design parameter values was studied under subcritical flow conditions. The performance of a TPKSW installed along a straight, rectangular channel was tested in a laboratory setting under fixed-bed and subcritical flow conditions. The main goals of this work were to (1) describe the hydraulic characteristics of a TPKSW flow (such as water surface profile, specific energy, and outflow efficiency); (2) offer a reliable evaluation of the discharge coefficient; (3) determine the suitability of the De Marchi, Domínguez and Schmidt methods, by comparing the results obtained for TPKSW; (4) find the outflow efficiency in comparison to the RPKSW, and (5) develop a useful and reliable equation for TPKSW which is a crucial requirement for applications.

2. BASIC THEORY

The discharge over the side weir per unit length, q , can be estimated using:

$$q = -\left(\frac{dQ}{dx}\right) = \left(\frac{dQ_w}{dx}\right) = \frac{2}{3} C_d \sqrt{2g} [y_1 - P]^{1.5} \tag{6}$$

where Q_w is the weir overflow discharge, y_1 is the flow depth at the upstream end of the side weir at channel center, and x is the distance from the beginning of the side weir. (y_1-P) is the piezometric head over the side weir.

2.1. De Marchi approach

Along the side weir, the equation for the closed form solution of the water surface differential was first presented by De Marchi, assuming constant energy in the main channel:

$$x = \frac{3}{2} \frac{b}{C_d} (\Phi_i - \Phi_{i-1}) \quad (7)$$

where Φ_i is given by:

$$\Phi_i = \frac{2E_i - 3P}{E_i - P} \sqrt{\frac{E_i - y_i}{y_i - P}} - 3 \sin^{-1} \left(\sqrt{\frac{E_i - y_i}{y_i - P}} \right) \quad (8)$$

Therefore, the relation between weir opening length (W) and other hydraulic variables of the flow is:

$$W = \frac{3}{2} \frac{b}{C_d} (\Phi_2 - \Phi_1) \quad (9)$$

where E is the specific energy and y is the flow depth in the main channel. Φ is the flow function of De Marchi. Equation (8) was first derived by De Marchi (1934) and can be used beneficially as a discharge equation for the side weir. Φ_1 and Φ_2 indicate upstream and downstream of the weir, respectively, and C_d is determined experimentally.

2.2. Schmidt approach

The Schmidt approach is valid where the flow arrives and continues in the river regime. The Poleni equation is used in the Schmidt approach (Schmidt, 1954):

$$Q_w = C_d \frac{2}{3} \sqrt{2g} W h_a^{3/2} \quad (10)$$

$$h_a = \frac{1}{2} (h_1 + h_2) \quad (11)$$

where h_a is the average piezometric head over the weir (m), h_1 is the piezometric head over the weir at the upstream end of the side weir (m), and h_2 is the piezometric head over the weir at the downstream end of the side weir (m).

2.3. Domínguez approach

The method developed by Domínguez provides a simple yet accurate way to determine the discharge of the side weir flow (Bagheri *et al.* 2014b). Assuming that specific energy along the side weir is constant and the water surface profile in the side weir changes linearly along the channel, the overflow discharge, Q_w (m^3/s), is given by:

$$Q_w = \left[\frac{2}{5} C_d \frac{\left(\frac{h_2}{h_1} \right)^{2.5} - 1}{\left(\frac{h_2}{h_1} \right) - 1} \right] \frac{2}{3} \sqrt{2g} W h_1^{1.5} \quad (12)$$

3. EXPERIMENTAL SETUP AND PROCEDURE

The experiments were conducted in a rectangular main channel (12 m long, 0.50 m wide and 0.50 deep) and a discharge evacuation channel (12 m long, 0.50 m wide and 0.70 deep). The bed slope of the main channel was 0.1%. The channels were made of a smooth, well painted steel bed with vertical glass sidewalls. The bed had an average Manning's roughness coefficient \bar{n} of 0.0099. A sluice gate was placed at the end of the main channel to control the depth of the flow. The width of the

evacuation channel across the side weir was 1.3 m and constructed in a circular to provide free overflow conditions. Figure 4 shows a scheme of the experimental setup.

A sharp-crested rectangular weir was placed at the end of the evacuation channel in order to measure the discharge of the side weir. A digital point gauge with ± 0.01 mm accuracy was placed upstream at a distance of 0.4 m from the sharp-crested weir. TPKSWs were fabricated from fully aerated steel plates with sharp edges. These were fixed flush to the main channel wall.

The water was fed to the main channel from a tank via a supply pipe under the influence of gravitational forces. The discharge was controlled by a valve and measured by an electromagnetic flow meter with an accuracy of ± 0.01 L/s. The results were compared to a calibrated 90° V-notched weir. The overflow discharge was measured via a calibrated standard rectangular weir, located at the downstream end of the evacuation channel. The water depth in the channel was measured using a digital point meter for steady-state flow conditions. For the water surface measurements, a measuring car was used on a rail that could move both along the side weir and across the main channel.

The experiments were carried out in the Hydraulic Laboratory at Firat University, Elazig, Turkey. The experiments were repeated under conditions of subcritical flow, steady-state flow, and free overflow, which frequently occur in most weir applications (such as rivers, irrigation, and land drainage systems). In all of the experiments, the piezometric head over the weir was greater than the required value for minimizing the surface tension effect (30 mm above the side weir height, as proposed by Novák & Cabelka 1981). TPKSW structures with different widths ($W = 0.25, 0.50$ and 0.75 m) and heights ($P = 0.12, 0.16$ and 0.20) were tested. The variation of discharge coefficient with respect to the Froude number, P/y_1 , W/b and W/L ratios was analyzed (Table 1). In total, 211 tests were carried out to study the behavior of the discharge coefficient.

4. RESULTS AND DISCUSSION

In this section, experimental results are presented and analyzed in order to describe the main features of the TPKSW flow and find the dimensionless parameters that primarily influence discharge capacity. The discharge coefficient of the TPKSW is named C_{PW} for ease of comparison, and the equations given for C_d in Section 1 are used. Some of the results along with the hydraulic and physical conditions of the experiments are presented in Table 2.

4.1. Assumption of constant specific energy

Since De Marchi equations were developed under constant specific energy assumptions, verification of the assumptions is required. Cross-sectional average flow velocities were calculated by using the flow depths measured at the upstream and downstream ends of the weir. The average specific energy was found using these velocities. Figure 5 illustrates that the average specific energy difference in the main channel between the two ends of the weir ($\Delta E = E_1 - E_2$) is 0.2%. Borghei *et al.* (1999) and Emiroglu *et al.* (2014) obtained a mean value of 3.7% and 1.0%, respectively. El-Khashab & Smith (1976) estimated a 5% value for subcritical flow. In this study, the energy difference is lower than 1.0% for all experiments involving TPKSW. Therefore, the specific energy is assumed to be constant.

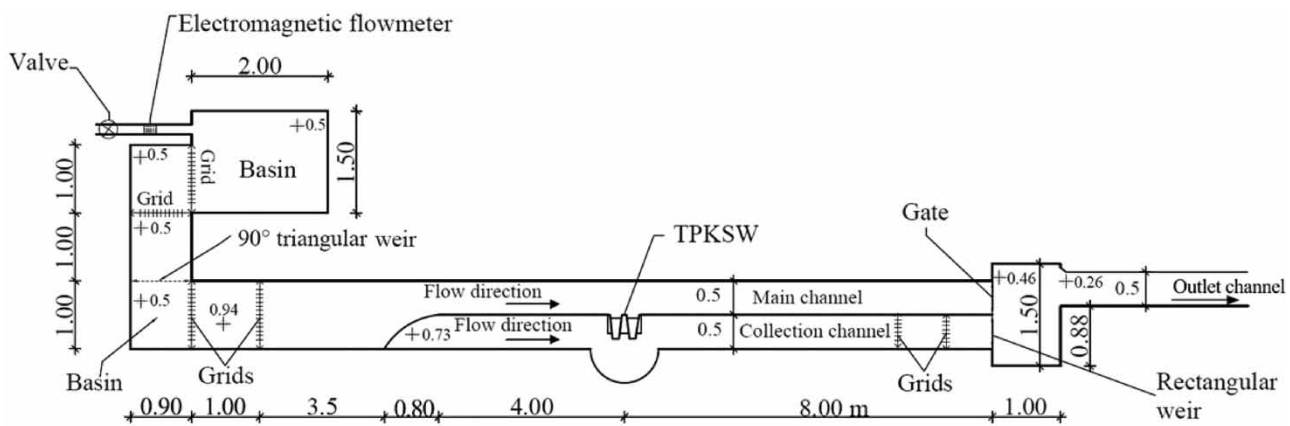


Figure 4 | Plan view of the experimental setup.

Table 1 | The range of variables used in the channel and TPKSW models

Variables	Limits of the value
The main channel width, b (m)	0.5
The main channel deep, z (m)	0.5
The main channel slope, J_0	0.001
Weir opening length, W (m)	0.25–0.50–0.75
Weir high, P (m)	0.12–0.16–0.20
Flow into the system, Q_1 (m ³ /s)	0.0119–0.1420
Froude number	0.12–0.87
Head, h_1 (m)	0.03–0.09
The inlet crest width W_i (m)	0.03–0.11
The outlet crest width W_o (m)	0.02–0.09
Length of sidewall B (m)	0.03–0.81
Downstream overhang length B_i (m)	0.13–0.40
Upstream overhang length B_o (m)	0
Wall thickness T_s (m)	0.002
Sidewall angle (°)	6

Table 2 | Conditions and results of tests for TPKSW

No.	W/b (-)	P (m)	L/W (-)	y_1 (m)	y_2 (m)	F_1 (-)	Q_1 (m ³ /s)	η (-)
1	1.00	0.12	4.82	0.1675	0.1960	0.7694	82.60	0.42
2	1.00	0.12	4.82	0.1696	0.1969	0.7681	84.00	0.35
3	1.00	0.12	4.82	0.1519	0.1555	0.2264	21.00	0.93
4	1.00	0.12	4.82	0.1728	0.1773	0.2862	32.20	0.94
5	1.00	0.12	4.82	0.1628	0.1701	0.3132	32.20	0.82
6	1.00	0.12	4.82	0.1574	0.1637	0.3293	32.20	0.82
7	1.00	0.12	4.82	0.1800	0.1884	0.3689	44.10	0.86
8	1.00	0.12	4.82	0.1644	0.1710	0.4225	44.10	0.69
9	1.00	0.16	4.82	0.1947	0.1997	0.2400	32.30	0.79
10	1.00	0.16	4.82	0.2057	0.2111	0.2636	38.50	0.82
11	1.00	0.16	4.82	0.2175	0.2237	0.2902	46.10	0.82
12	1.00	0.16	4.82	0.2038	0.2116	0.3201	46.10	0.72
13	1.00	0.16	4.82	0.2021	0.2098	0.3387	48.20	0.71
14	1.00	0.16	4.82	0.2016	0.2067	0.4084	57.90	0.61
15	1.00	0.16	4.82	0.2032	0.2052	0.4197	60.20	0.60
16	1.00	0.20	4.82	0.2350	0.2388	0.1884	33.60	0.75
17	1.00	0.20	4.82	0.2419	0.2602	0.4760	88.70	0.39
18	1.00	0.20	4.82	0.2453	0.2619	0.5184	98.60	0.35
19	1.00	0.20	4.82	0.2350	0.2559	0.6002	107.10	0.28
20	1.00	0.20	4.82	0.2311	0.2542	0.6485	112.80	0.32
21	1.00	0.20	4.82	0.2343	0.2606	0.6809	120.90	0.26
22	1.00	0.20	4.82	0.2331	0.2374	0.2015	35.50	0.84

(Continued.)

Table 2 | Continued

No.	W/b (-)	P (m)	L/W (-)	y_1 (m)	y_2 (m)	F_1 (-)	Q_1 (m ³ /s)	η (-)
23	0.50	0.12	4.82	0.1882	0.1903	0.1729	22.10	0.73
24	0.50	0.12	4.82	0.1734	0.1734	0.1530	17.30	0.68
25	0.50	0.12	4.82	0.1512	0.1529	0.1293	11.90	0.54
26	0.50	0.12	4.82	0.1796	0.1828	0.2878	34.30	0.41
27	0.50	0.12	4.82	0.1684	0.1716	0.3170	34.30	0.32
28	0.50	0.16	4.82	0.1994	0.2014	0.1413	19.70	0.67
29	0.50	0.16	4.82	0.1901	0.1913	0.1518	19.70	0.48
30	0.50	0.16	4.82	0.1962	0.1984	0.1322	18.00	0.65
31	0.50	0.16	4.82	0.2136	0.2151	0.1792	27.70	0.56
32	0.50	0.16	4.82	0.1973	0.1995	0.2018	27.70	0.42
33	0.50	0.20	4.82	0.2582	0.2598	0.1246	25.60	0.69
34	0.50	0.20	4.82	0.2384	0.2409	0.1405	25.60	0.46
35	0.50	0.20	4.82	0.2475	0.2491	0.1826	35.20	0.42
36	0.50	0.20	4.82	0.2311	0.2335	0.2023	35.20	0.28
37	0.50	0.20	4.82	0.2585	0.2623	0.2333	48.00	0.39
38	1.50	0.12	4.82	0.1501	0.1589	0.4006	36.50	0.85
39	1.50	0.12	4.82	0.1500	0.1572	0.3451	31.40	0.97
40	1.50	0.12	4.82	0.1552	0.1656	0.4480	42.90	0.85
41	1.50	0.12	4.82	0.1527	0.1627	0.4593	42.90	0.78
42	1.50	0.16	4.82	0.1900	0.1957	0.2907	37.70	0.93
43	1.50	0.16	4.82	0.1939	0.2023	0.3485	46.60	0.85
44	1.50	0.16	4.82	0.1939	0.2063	0.4121	55.10	0.74
45	1.50	0.16	4.82	0.1949	0.2085	0.4503	60.70	0.69
46	1.50	0.16	4.82	0.1937	0.2099	0.4946	66.00	0.63
47	1.50	0.20	4.82	0.2300	0.2343	0.2217	38.30	0.92
48	1.50	0.20	4.82	0.2401	0.2470	0.2795	51.50	0.92
49	1.50	0.20	4.82	0.2339	0.2419	0.2907	51.50	0.80
50	1.50	0.20	4.82	0.2426	0.2549	0.3734	69.90	0.73
51	1.50	0.20	4.82	0.2339	0.2472	0.3945	69.90	0.63

4.2. Water surface profile

The water surface profiles were measured at 18 points along the center of the main channel and along the side weir. In addition to the existing data, water surface profiles were generated by calculating intermediate values with the extrapolation method (Figures 6 and 7). The water level over the TPKSW generally dropped sharply at the upstream end of the side weir, due to acceleration induced by the lateral flow, and then ascended downstream. This rising profile is compatible with the principle of spatially varied flow over side weirs. Similar actions have been seen for subcritical flow over trapezoidal sharp-crested side weirs and triangular labyrinth side weirs (e.g., Emiroglu *et al.* 2010; Ghaderi *et al.* 2020). Increasing the Froude number increases the flow velocity and makes it difficult to divert the flow to the side weir. Therefore, increasing the Froude number increases the difference between upstream and downstream water levels. The effect of the Froude number is also in agreement with the theory of spatially varied flow over side weirs. It was observed that the water level fell in two regions above the TPKSW, especially in conditions with large Froude numbers. The regions are above the inlet keys. The flow rate decreases at the entrance of the inlet key and thus helps flow uniformity. Karimi *et al.* (2018) experimentally demonstrated that a similar situation occurs for RPKSW.

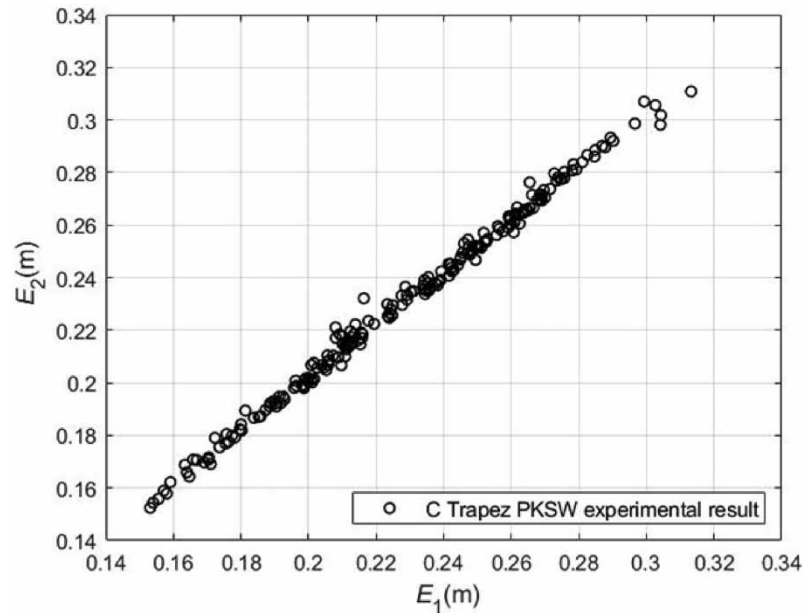


Figure 5 | Specific energy at the ends of the TPKSW.

4.3. Discharge coefficient of trapezoidal piano key side weir using different approaches

Figure 8 shows that the flow coefficient values obtained using the Schmidt and Domínguez methods are quite compatible with each other. Similarly, Emiroglu *et al.* (2010) stated that the data obtained by the Schmidt and Domínguez methods for the triangular labyrinth side weir almost overlap with each other. In the current study, compared to the De Marchi method, the other two methods have more scattered results, as presented in Figure 8. Between the De Marchi method and other methods, there is 71 and 89% agreement for $F_1 = 0.2$ and $F_1 = 0.8$, respectively. Contrary to the current study, in Emiroglu *et al.* (2016), the data obtained with the De Marchi method were more scattered and closer to the data of the Schmidt and Domínguez methods.

It was observed that the discharge coefficient decreases as the Froude number increases for all approaches (see Figure 8). Mehri *et al.* (2018) used the De Marchi approach in their study for low Froude numbers (0.05–0.30) and obtained a decreasing trend in some experiments and an increasing trend in other experiments, between F_1 and C_{PW} . Moreover, the data obtained by the De Marchi method were very scattered. However, a decreasing trend was obtained between F_1 - C_{PW} in the studies that used the De Marchi method (Borghei *et al.* 1999, 2013; Emiroglu *et al.* 2014). Different from other studies, this study provides a better understanding of the relationship between F_1 and C_{PW} by performing experiments over a wide range of Froude numbers. Bagheri *et al.* (2014a, 2014b) stated that the Domínguez method provides reliable results in a sharp-edged weir. In addition, Emiroglu & Ikinçiogullari (2016) showed that the Schmidt method is reliable for conventional side weirs. Similarly, all approaches provide reasonable results for TPKSW in the present study.

4.4. Effects of upstream head

As the head (h_1) approaches a certain value, the effective weir length gradually decreases and, eventually, the behavior of the TPKSW converges with the behavior of a linear weir. When the piezometric head over the weir is small, the flow falls freely over the full length of the weir. Crookston & Tullis (2011) stated that there is no significant gain for $h_1/P > 1.0$ at the frontal labyrinth weirs. According to studies conducted for PKW, small head values maximize the contribution of increased crest length (L) (Lempérière *et al.* 2011; Anderson & Tullis 2013). Similarly, Figure 9 shows that the discharge coefficient is a decreasing function of the h_1/P value. The rate of change of C_{PW} decreases as h_1/P increases. The trend of C_{PW} as a function of h_1/P is in agreement with previous studies conducted for different types of side weirs (Singh *et al.* 1994; Jalili & Borghei 1996; Borghei *et al.* 1999; Emiroglu *et al.* 2011; Abbasi *et al.* 2020).

In this study, head value is between $3 < h_1 < 9$ cm, which corresponds with the range of $0.15 < h_1/P < 0.57$. For $W/b = 0.5$, $P/W = 0.64$ gives higher C_{PW} values of TPKSW, compared to P/W values of 0.48 and 0.80. In the range of $0.2 \leq h_1/P \leq 0.5$,

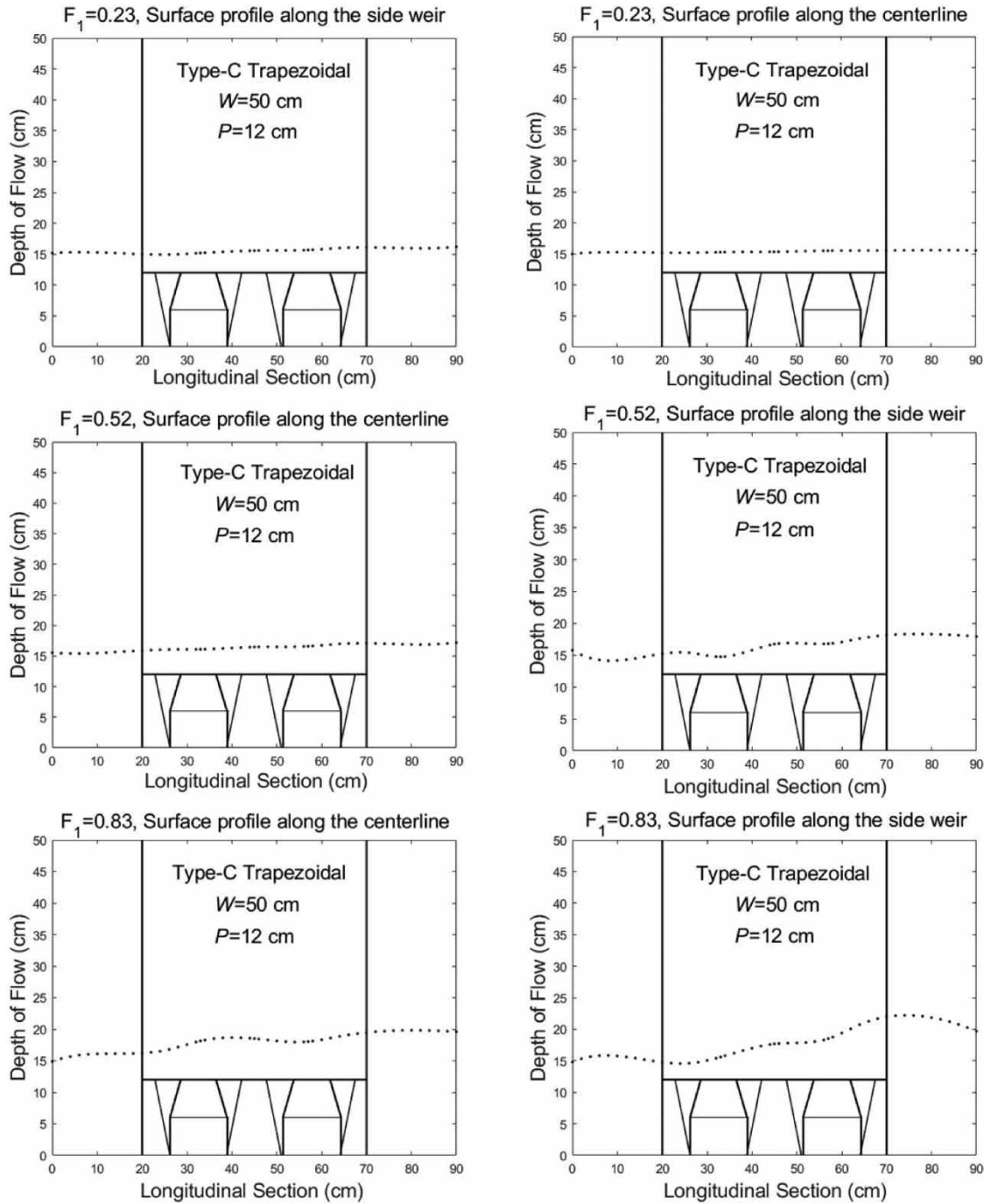


Figure 6 | Water surface profile for $P = 0.12$ m TPKSW.

the most stable behavior of C_{PW} is observed at $P/W = 0.80$, with an average slope value of -0.15 . A mean slope of -0.44 for $P/W = 0.48$ and -0.80 for $P/W = 0.64$ is observed. For a given value of h_1 , C_{PW} increases as crest height increases. The reason for this behavior is the fact that it has a wider inlet key cross-sectional area. As a result, the velocity decreases as the flow approaches the side weir and the flow becomes uniform.

4.5. Effects of upstream Froude number

For all TPKSW models, the relation between C_{PW} and Froude number is in the form of $C_{PW} = aF_1^b$. In all cases, the b takes negative values, therefore C_{PW} is a decreasing function of the Froude number. Similar behaviors are observed in labyrinth side

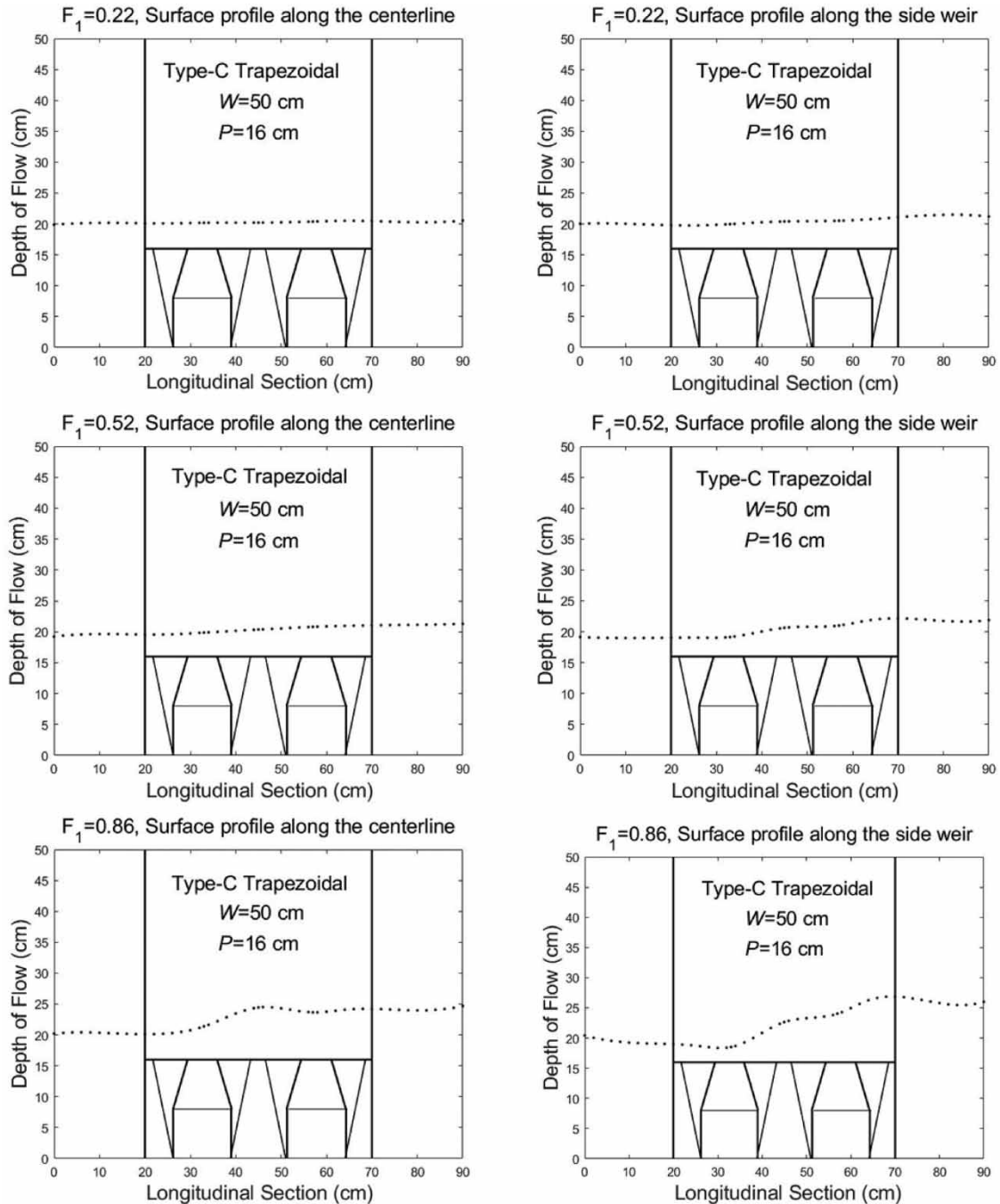


Figure 7 | Water surface profile for $P = 0.16$ m TPKS. W.

weirs (Aydın & Emiroglu 2016; Abbasi *et al.* 2020) and in the curved channel RPKSW (Mehri *et al.* 2018). Figure 10 presents the flow coefficient as a function of Froude number. The flow coefficient is a decreasing function of the Froude number. The lowest discharge coefficients were observed at $P/W = 0.64$ and $P/W = 0.48$, respectively (Figure 10(a)). For $W/b = 1.0$, $P/W = 0.32$ provides the most stable results at low and high Froude numbers, with a slope of -0.32 at $F_1 = 0.2$, and -0.10 for $F_1 = 0.6$. For $P/W = 0.24$, the slope is equal to -0.46 at $F_1 = 0.2$ and -0.14 at $F_1 = 0.6$. In the experiments carried out for $W/b = 1.5$, the amount of discharged flow is too much for the capacity of the collection channel. When the flow rate entering the system increases, in order to obtain the desired flow depths, the tail water rises and exceeds the weir crest.

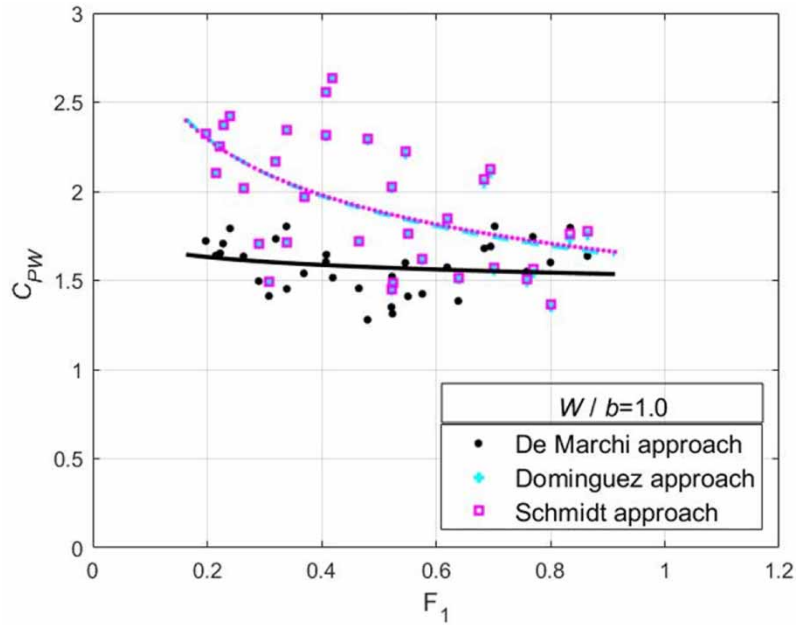


Figure 8 | Discharge coefficient of TPKSW according to different approaches.

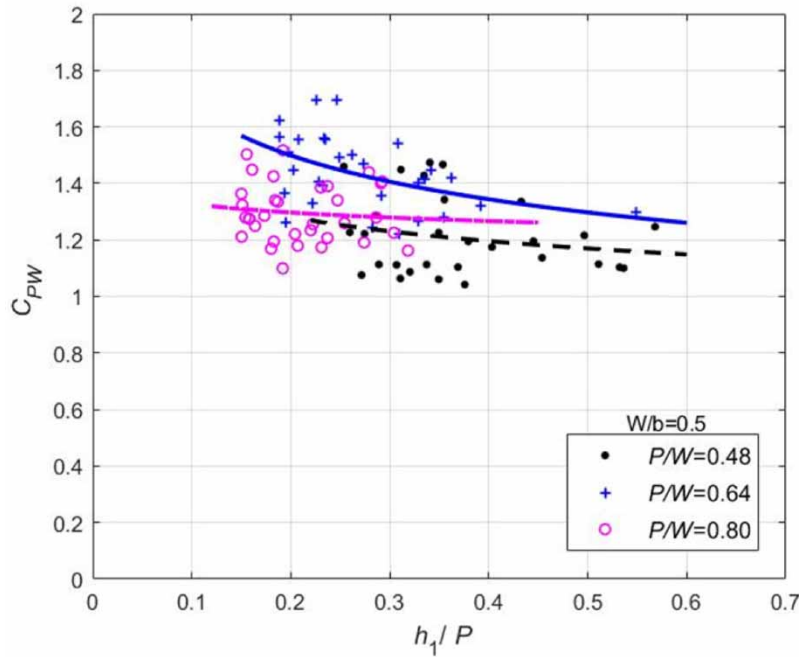


Figure 9 | Values of C_{PW} versus h_1/P for TPKSW (a) $W/b = 0.5$, (b) $W/b = 1.0$, (c) $W/b = 1.5$.

Few experiments have been possible under these conditions. Missing data are predicted by the extrapolation method. Figure 10(c) shows that, for low Froude number values, $P/W = 0.21$ provides the highest and $P/W = 0.16$ gives the lowest C_{PW} . It is seen that the Froude number is more effective on C_{PW} at $P/W = 0.16$. At high Froude numbers, the best performance is obtained at $P/W = 0.27$ and the effect of the F_1 number decreases. The ineffective region at the corners of the keys

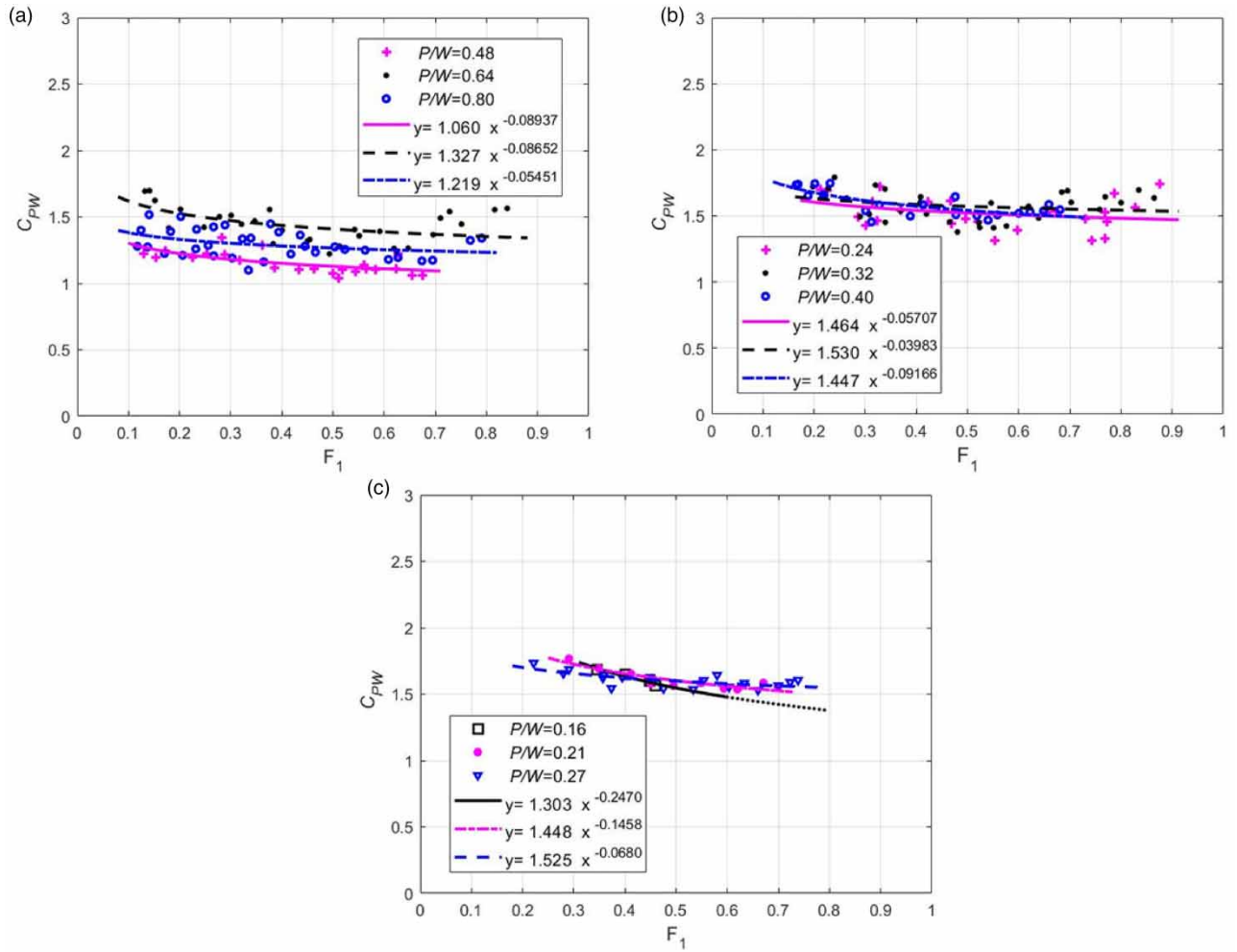


Figure 10 | (a–c) C_{PW} versus F_1 for different dimensionless weir lengths of TPKSW (a) $W/b = 0.5$, (b) $W/b = 1.0$, (c) $W/b = 1.5$.

expands and lowers the outflow discharge when F_1 value is raised (see Figure 11). In the case of large F_1 values, (starting from the upstream) in all of the 1st half outlet key crest and a certain part of the 1st side wall of the TPKSW do not provide discharge (see Figure 11). This is due to the fact that the velocity of the flow increases as the flow rate in the main channel is increased. With larger velocity vectors, changing direction of the flow to the side weir becomes harder.

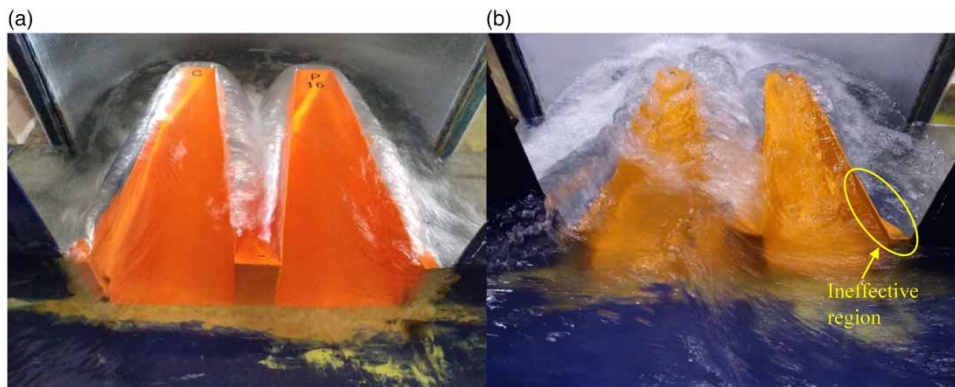


Figure 11 | Change of flow on TPKSW depending on F_1 (a) $F_1 = 0.22$, and (b) $F_1 = 0.76$.

4.6. Outflow efficiency

Outflow efficiency is defined as:

$$\eta = \frac{Q_w}{Q_1} \quad (13)$$

η is correlated with the dimensionless parameter χ :

$$\chi = \frac{(1/F_2)}{(P/y_2)} \quad (14)$$

where F_2 is the downstream Froude number and y_2 is the depth in the main channel at the downstream end of a linear side weir. Figure 12 shows η versus χ for rectangular and TPKSWs with different W/b ratios. The discharge efficiency η is an increasing function of χ and can be expressed as $\eta = a\chi^b$ with a correlation coefficient above 0.95. For a fixed P/y_2 value, η decreases with increasing F_2 . Similarly, if the F_2 value is constant, the η values decrease as the P/y_2 value increases. Maranzoni *et al.* (2017) obtained similar findings for the short-crested side weir in a converging channel. It was observed that the η increases with an increase in the W/b ratio, and there is no significant change depending on the crest height (see Figure 12). The results are in agreement with the findings obtained for type C rectangular PKSW (Karimi *et al.* 2018). The design introduced in Karimi *et al.* (2018) was found to be slightly more efficient, compared to the current study in the range of $0 < \chi < 12$, where χ is very small. This occurs from the relationship between increasing values of either F_2 or P/y_2 . In this range, the PKSW model starts with the inlet key upstream of the side weir opening. This provides an advantage by increasing the efficiency of the upstream part of the weir, where lateral flow effects with high velocity are dominant.

4.7. Comparison with literature

Subramanya & Awasthy (1972), Hager (1987) and Borghei *et al.* (1999) developed empirical formulas for the flow coefficient C_d in the case of rectangular weir lateral flow in a linear channel. The discharge coefficient C_d was calculated by using Equations (1)–(3) and comparing them with the C type TPKSW data generated in the current study. With the increase of Froude number value, the discharge coefficients of both TPKSW and rectangular side weirs decrease in a similar trend. The ratio of the discharge coefficient of TPKSW to the discharge coefficient of the rectangular side weir was found to be between 2.9 and 12 (Figure 13). The TPKSW effective crest length is equal to 4.82 times the weir opening. Therefore, a positive effect of the increased weir length on the discharge efficiency is observed. At large values of the Froude number, the TPKSW achieves a very significant increase in flow coefficient compared to rectangular weirs. This difference is too large to be explained by the contribution of effective weir length only, reflecting that the hydraulic behavior of piano key weirs in lateral flow is quite different from the behavior of rectangular side weirs. The secondary flow in TPKSWs which is the cause by lateral flow is more severe as in trapezoidal labyrinth side weirs compared to rectangular side weirs (Emiroglu *et al.* 2014). Intensity of secondary movement increases with increasing overflow length. As the relative side weir length grows, an increase in the secondary flow causes an increase in the deflection angle and change in momentum towards the side weir. The intensity of the secondary flow occurring inside the side weir decreases as the flow velocity inside the side weir reduces (Abbasi *et al.* 2020).

The effects of h_1/P on discharge coefficients of the trapezoidal labyrinth side weir, triangular labyrinth side weir and TPKSW are similar (Figure 14(a)). For constant crest height and small head values, the discharge coefficient of trapezoidal labyrinth side weir is greater than C_{PW} . As head increases, PKSW and trapezoidal labyrinth side weir discharge coefficients get very close to each other. C_{PW} over C_d (triangular labyrinth side weir) was found to be 2.1. C_{PW} over C_d (trapezoidal labyrinth side weir) was found to be between 0.92 and 1. The triangular labyrinth side weir data are calculated using Equation (4). The weirs used in all three studies consist of two units and $W/b = 1.0$. Figure 14(b) presents the relationship between Froude number and the discharge coefficient. Increasing the Froude number decreases the discharge coefficient of the PKSW. Conversely discharge coefficients of the trapezoidal labyrinth and triangular labyrinth side weirs increase. The highest discharge coefficients are observed in the trapezoidal labyrinth weir. The lowest values of the discharge coefficients were observed in the triangular labyrinth weir. Considering that the ratio of effective weir length (L) to weir opening (W) of TPKSW is $L/W = 4.82$, the discharge coefficients of the trapezoidal labyrinth weir are quite high compared to TPKSW. The most significant

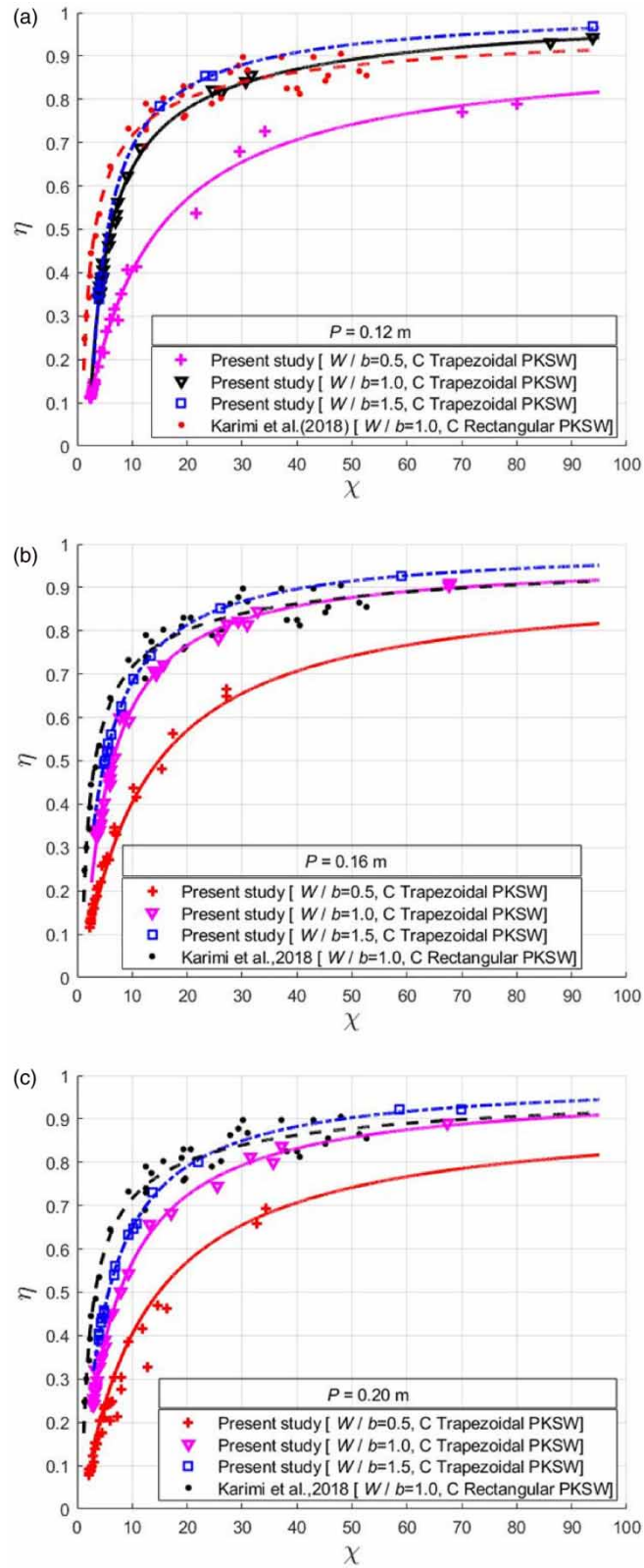


Figure 12 | Outflow efficiency of TPKSW (a) $P = 0.12$ m, (b) $P = 0.16$ m, (c) $P = 0.20$ m.

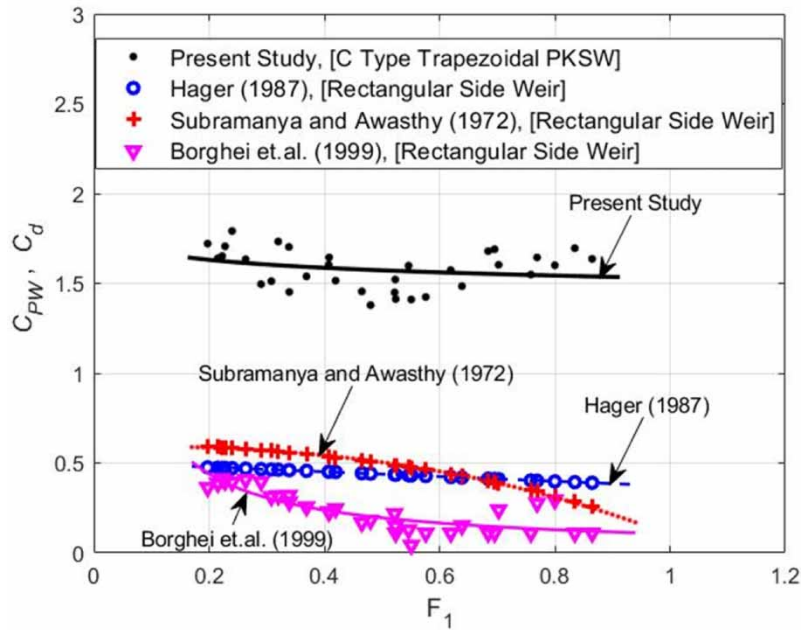


Figure 13 | Comparison of a TPKSW with a rectangular side weir.

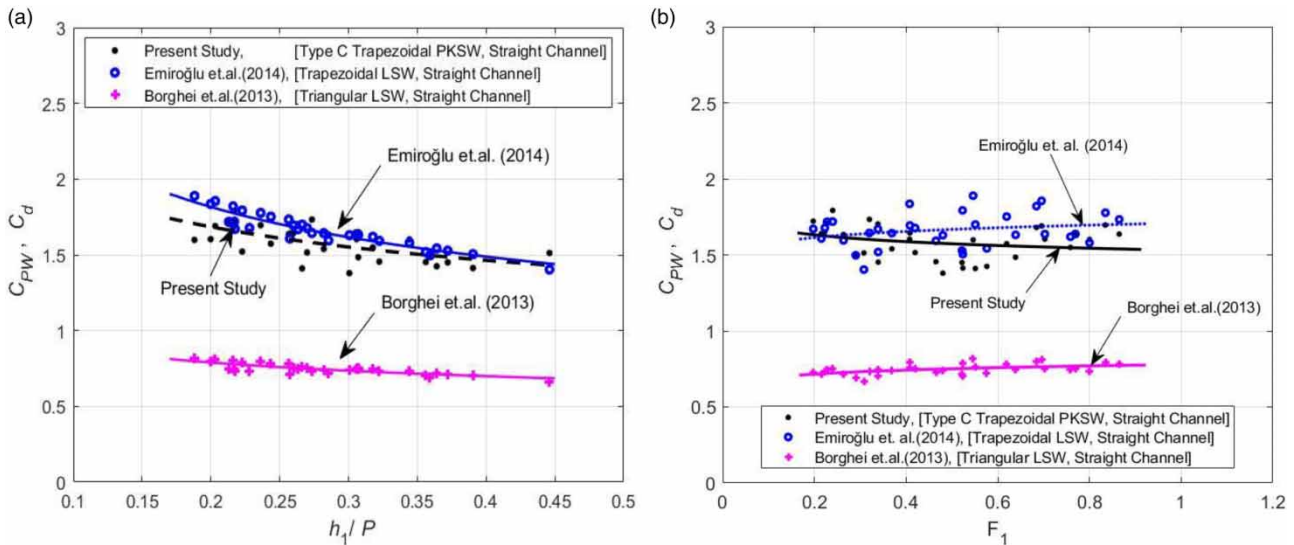


Figure 14 | (a, b) Comparison of TPKSW with trapezoidal and triangular labyrinth side weirs.

difference between the labyrinth weir and PKSW geometries is the inlet and outlet key ramps in the PKSW. This suggests that the performance difference between the two weir models is related to the slopes of the ramps. Higher velocities are required to fill the inlet key and to reach crest of outlet key due to the presence of ramps. It is expected that the decrease in the slope of the inlet key contributes to the discharge capacity. However, increasing the slope of the outlet key improves the discharge as the velocity increases.

4.8. Proposed equation for calculating the weir discharge coefficient

In this study, by using the results of the Domínguez approach and nonlinear regression analysis, Equation (15) is developed for the discharge coefficient of TPKSW. As presented in Figure 15, the weir discharge coefficient is successfully predicted for

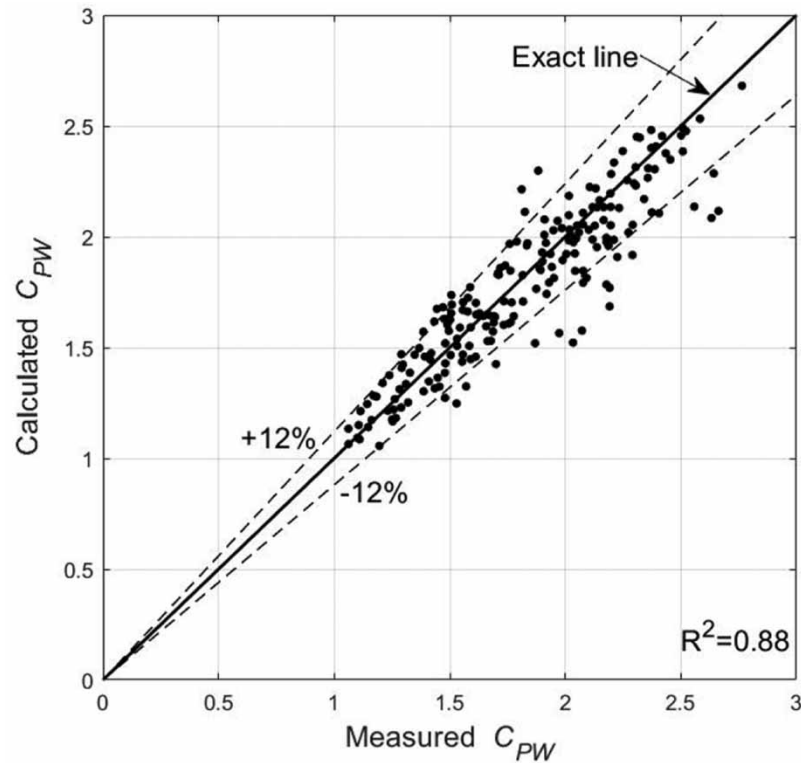


Figure 15 | Comparison of measured C_{PW} values with those calculated from Equation (15).

the experimental conditions. To evaluate the accuracy of the estimation using the nonlinear model, the root-mean square error (RMSE) and coefficient of determination (R^2) criteria were used. For Equation (15), RMSE and R^2 are 0.16968 and 0.88, respectively. Figure 15 compares the measured C_{PW} values with those predicted by Equation (15). Good correlation was observed between the measured values and the values computed from the equation. Thus, a reliable equation is introduced for the discharge coefficient of a two unit TPKSW located on a straight channel in subcritical flow conditions:

$$C_{PW} = \left(-13.169 + \left(\frac{n}{P} \right)^{0.888} \right) \left(14.012 + \left(\frac{h_1}{P} \right)^{-0.764} \right) \left(-0.687 + \left(\frac{H_1}{P} \right)^{-0.243} \right) \\ (1.322 + (F_1)^{0.421}) \left(\frac{B}{P} \right)^{-4.110} \left(0.046 + \left(\frac{B_i}{P} \right)^{1.692} \right) \left(-0.135 + \left(\frac{W}{P} \right)^{1.858} \right) \quad (15)$$

Equation (15) is subject to the limitations of present tests: $0.13 \leq F_1 \leq 0.88$, $0.17 \leq H_1/P \leq 0.85$, $0.5 \leq W/b \leq 1.5$, $1.4 \leq B/P \leq 6.73$, $0.15 \leq h_1/P \leq 0.57$, $W_i/W_o = 1.23$, $n = L/W = 4.83$, and $\alpha = 6^\circ$.

5. CONCLUSIONS

In the current study, the hydraulic characteristics of a TPKSW were experimentally studied. The values of discharge coefficient for TPKSW were obtained using De Marchi, Schmidt and Domínguez approaches. The study leads to the primary results listed below:

- The fundamental constant energy assumption commonly used in side weir flow modeling is valid for TPKSW flow.
- The location of the low levels observed in the water surface profile shows that the contribution of the inlet key to the discharge capacity is higher compared to the other TPKSW parts as in frontal flow.
- Contrary to the frontal weir, in the case of lateral flow, the positions of the inlet and outlet keys along the weir are more effective for the behavior of the flow.

- (d) As the P/W value increases, the flow coefficient increases up to a certain value (0.64) and then decreases. Key slopes should be optimized for new TPKSW designs since the change in key slopes is effective.
- (e) In comparison to the traditional rectangular side weir and triangular labyrinth side weir discharge coefficients, the TPKSW discharge coefficient has greater values.
- (f) A higher discharge capacity is observed in the trapezoidal labyrinth side weir compared to TPKSW especially for $0.38 < F_1 < 0.76$.

DATA AVAILABILITY STATEMENT

All relevant data are included in the paper or its Supplementary Information.

CONFLICT OF INTEREST

The authors declare there is no conflict.

REFERENCES

- Abbasi, S., Fatemi, S., Ghaderi, A. & Di Francesco, S. 2020 The effect of geometric parameters of the antivortex on a triangular labyrinth side weir. *Water* **13** (1), 14.
- Anderson, R. M. & Tullis, B. 2011 Influence of Piano Key Weir Geometry on Discharge. In *Proceedings Int. Conference Labyrinth and Piano Key Weirs*, pp. 75–80.
- Anderson, R. M. & Tullis, B. 2013 Piano key weir hydraulics and labyrinth weir comparison. *Journal of Irrigation Drainage Engineering* **139**, 246–253.
- Aydin, M. C. & Emiroglu, M. E. 2013 Determination of capacity of labyrinth side weir by CFD. *Flow Measurement Instruments* **29**, 1–8.
- Aydin, M. C. & Emiroglu, M. E. 2016 Numerical analysis of subcritical flow over two-cycle trapezoidal labyrinth side weir. *Flow Measurement Instruments* **48**, 20–28.
- Bagheri, S., Kabiri-Samani, A. R. & Heidarpour, M. 2014a Discharge coefficient of rectangular sharp-crested side weirs, part I: traditional weir equation. *Flow Measurement Instruments* **35**, 109–115.
- Bagheri, S., Kabiri-Samani, A. R. & Heidarpour, M. 2014b Discharge coefficient of rectangular sharp-crested side weirs, part II: Domínguez's method. *Flow Measurement Instruments* **35**, 116–121.
- Borghei, S. M. & Parvaneh, A. 2011 Discharge characteristics of a modified oblique side weir in subcritical flow. *Flow Measurement Instruments* **22**, 370–376.
- Borghei, M., Jalili, M. R. & Ghodsian, M. 1999 Discharge coefficient for sharp-crested side weir in subcritical flow. *Journal Hydraulic Engineering* **125**, 1051–1056.
- Borghei, S. M., Nekooie, M. A., Sadeghian, H. & Ghazizadeh, M. R. J. 2013 Triangular labyrinth side weirs with one and two cycles. *Water Management* **166**, 27–42.
- Crookston, B. M. & Tullis, B. P. 2011 The design and analysis of labyrinth weirs. In: *31st Annual USSD Conference*, pp. 1661–1681.
- De Marchi, G. 1934 Essay on the performance of lateral weirs. *L' Energia Elettrica* **11**, 849–860.
- Domínguez, F. J. 1935 Hidráulica. (Hydraulics). 1st ed. Nascimento editor, Santiago, Chile.
- El-Khashab, A. M. M. & Smith, K. V. H. 1976 Experimental investigation of flow over side weirs. *Journal of Hydraulic Division* **102**, 1255–1268.
- Emiroglu, M. E. & Ikinçiogullari, E. 2016 Determination of discharge capacity of rectangular side weirs using Schmidt approach. *Flow Measurement Instruments* **50**, 158–168.
- Emiroglu, M. E., Kaya, N. & Ozturk, M. 2007 Investigation of Labyrinth Side Weir Flow and Scouring at the Lateral Intake Region in A Curved Channel. The Scientific and Technological Research Council of Turkey, Engineering Science Research Grant Group, Project 104M394, p. 253.
- Emiroglu, M. E., Kaya, N. & Agaccioglu, H. 2010 Discharge capacity of labyrinth side weir located on a straight channel. *Journal of Irrigation Drainage Engineering* **136**, 37–46.
- Emiroglu, M. E., Agaccioglu, H. & Kaya, N. 2011 Discharging capacity of rectangular side weirs in straight open channels. *Flow Measurement Instrumentation* **22**, 319–330.
- Emiroglu, M. E., Aydin, M. C. & Kaya, N. 2014 Discharge characteristics of a trapezoidal labyrinth side weir with one and two cycles in subcritical flow. *Journal of Irrigation Drainage Engineering* **140**, 401–407.
- Emiroglu, M. E., Tunç, M. & Ikinçiogullari, E. 2016 Determination of discharge capacity at the triangular labyrinth side weirs using different approaches. In *10th ICOLD European Club Symposium*.
- Ghaderi, A., Dasineh, M., Abbasi, S. & Abraham, J. 2020 Investigation of trapezoidal sharp-crested side weir discharge coefficients under subcritical flow regimes using CFD. *Applied Water Science* **10** (1), 1–12.
- Gharibvand, R., Heidarnejad, M., Kashkouli, H., Hasoonizadeh, H. & Kamanbedast, A. A. 2016 A laboratory study into hydraulic coefficient in trapezoidal labyrinth weir and piano key weir. *Fresenius Environmental Bulletin* **25** (12), 5590–5598.

- Hager, W. H. 1987 Lateral outflow over side weirs. *Journal of Irrigation Drainage Engineering* **113**, 491–504.
- Jalili, M. R. & Borghei, S. M. 1996 Discussion of discharge coefficient of rectangular side weirs. *Journal of Irrigation Drainage Engineering* **122**, 132–140.
- Kabiri-Samani, A. & Javaheri, A. 2012 Discharge coefficients for free and submerged flow over piano key weirs. *Journal of Hydraulic Research* **50** (1), 114–120.
- Karimi, M., Attari, J., Saneie, M. & Jalili Ghazizadeh, M. R. 2018 Side weir flow characteristics comparison of piano key, labyrinth, and linear types. *Journal Hydraulic Engineering* **144**, 12.
- Kumar, C. P. & Pathak, S. K. 1987 Triangular side weirs. *Journal of Irrigation Drainage Engineering* **113**, 1–12.
- Leite Ribeiro, M., Bieri, M., Boillat, J. L., Schleiss, A. J. & Sharma, N. 2012 Discharge capacity of piano key weir. *Journal of Hydraulic Engineering* **138**, 943–950.
- Lempérière, F., Vigny, J. P. & Ouamane, A. 2011 General comments on Labyrinth and Piano Key Weirs: The past and present. In *Proceedings Int. Conference Labyrinth and Piano Key Weirs*, pp. 17–24.
- Maranzoni, A., Pilotti, M. & Tomirotti, M. 2017 Experimental and numerical analysis of side weir flows in a converging channel. *Journal Hydraulic Engineering* **143**, 04017009.
- Mehri, Y., Soltani, J., Saneie, M. & Rostami, M. C. 2018 Discharge coefficient of a C-type piano key side weir at 30 degrees and 120 degrees sections of a curved channel. *Civil Engineering Journal of Tehran* **4**, 1702–1713.
- Mehri, Y., Esmaeili, S. & Soltani, J. 2020 Experimental study and performance comparison on various types of rectangular piano key side weirs at a 120 degrees section of a 180 degrees curved channel. *Applied Water Science* **10** (10), 1–13.
- Nezami, F., Davood, F. & Nekooie, M. A. 2015 Discharge coefficient for trapezoidal side weir. *Alexandria Engineering Journal* **54**, 595–605.
- Novák, P. & Cabelka, J. 1981 Models in hydraulic engineering; physical principles and design applications. *Monographs & Surveys in Water Resources Engineering*. Book ISBN: 0273084364 9780273084365. pp. 1-459.
- Ouamane, A. & Lempérière, F. 2006 Design of a new economic shape of weir. Proceedings of the international symposium on dams in the societies of the 21st century. *International Commission on Large Dams (ICOLD)* pp. 463–470.
- Pralong, J., Vermeulen, J., Blancher, B. & Laugier, F. 2011 A naming convention for the piano key weirs geometrical parameters. In *Proceedings Int. Conference Labyrinth and Piano Key Weirs*, pp. 271–278.
- Ranga Raju, K. G., Prasad, B. & Gupta, S. K. 1979 Side weir in rectangular channels. *Journal of Hydrological Engineering* **105** (5), 547–554.
- Saghari, A., Saneie, M. & Hosseini, K. 2019 Experimental study of one-and two-cycle trapezoidal piano-key side weirs in a curved channel. *Water Supply* **19**, 1597–1603.
- Schmidt, M. 1954 Zur frage des abflusses uber streichwehre, Techniv Berlin Charlottenbury. *Mitteilung NY41*, 1–68.
- Singh, R., Manivannan, D. & Satyanarayana, T. 1994 Discharge coefficient of rectangular side weirs. *Journal of Irrigation Drainage Engineering* **120**, 814–819.
- Subramanya, K. & Awasthy, S. C. 1972 Spatially varied flow over side weirs. *Journal of Hydraulic Division* **98**, 1–10.

First received 24 March 2022; accepted in revised form 5 July 2022. Available online 14 July 2022